Optimal Path Planning based on Annular Space Decomposition for AUVs Operating in a Variable Environment

Zheng Zeng, Andrew Lammas, Karl Sammut, Fangpo He
School of Computer Science, Engineering and Mathematics
Flinders University
Adelaide, Australia
{zheng.zeng, andrew.lammas, karl.sammut, fangpo.he}@flinders.edu.au

Abstract*—This paper presents an optimal and efficient path planner based on an annular space decomposition (ASD) scheme for Autonomous Underwater Vehicles (AUVs) operating in turbulent, cluttered and uncertain environments. The proposed scheme decomposes the search space into annular regions, and allows placing one or more control points within each of this region. The trajectory is then generated from this set of control points by using Splines. This arrangement gives more freedom to the placement of the control points, while still restricting the search space to reduce computation time. The ASD scheme has been integrated with both the Genetic Algorithm and the Quantum-behaved Particle Swarm Optimization based path planner and tested to generate an optimal trajectory for an AUV travelling through a turbulent ocean field in the presence of obstacles located with positioning uncertainty. Simulation results show that the resulting approach is able to obtain a more optimized trajectory than the concentric circle constrained method, and has faster convergence speed and use less computation time than the unconstrained full space searching method. Monte Carlo simulations demonstrate the robustness and superiority of the proposed ASD scheme compared with the other two schemes.

Keywords - path planning; optimization; space decomposition; evolutionary algorithm; particle swarm optimization;

I. INTRODUCTION

AUVs are increasingly being used to operate in dynamic, cluttered, and uncertain ocean environments. Real-Time Path planning is one of the most essential features required to ensure safe operation of a vehicle in such environments. An efficient path planner should be able to rapidly react to fast changing environments and generate a trajectory that leads the AUV from its initial or current position to its destination without encountering any obstacles or hazardous areas.

Path planning for AUVs is a topic that has been widely researched in recent years. Existing schemes typically use evolutionary algorithms to identify optimal trajectories through turbulent environments. Genetic Algorithm (GA) and Particle Swarm Optimization (PSO) are two well-known forms of evolutionary algorithms that are generally recognized to be effective and efficient optimization techniques for solving path planning problems. Alvarez [1] proposed a GA based path planner for AUVs in a variable ocean environment, with the assumption that all the paths are strictly monotonic with respect to the x-coordinate, while the y-coordinates are set up as the chromosome genes for the evolutionary algorithm. Zheng [2] and Nikolos [3] developed GA based route planners for unmanned aerial vehicles, but unlike Alvarez's work, the trajectories are represented using B-Splines where the coordinates of the spline control points form the chromosome genes. The control points can be freely located anywhere in the search space [2], [3]. This scheme is flawed, however, because there is no clear division of search work among the control points, thus the evolutionary algorithm attempts to search the whole space with every individual control point which is inefficient.

In order to save computation time, the points can be constrained to lie, for example, on deterministically spaced concentric circles, one control point per circle, radiating out from the start point to the destination [4]. However, this decomposition method distorts the search space since the area between neighbouring circles is unreachable, consequently the obtained path solution is usually suboptimal. Moreover, this approach limits the flexibility of the planner to plot optimal paths around obstacles.

An alternative control point placement method, herein referred to as Annular Space Decomposition (ASD) scheme, is proposed in this paper to facilitate more efficient searching and greater flexible placement of the control points. The ASD scheme decomposes the search space into multiple annular regions radiating out from the start point to the destination, with one or more control points allocated to each annulus. This arrangement gives more freedom to the placement of the control points, but still restricts the search space for each control point to its respective annulus to save computation time.

Similar to GA, PSO is also a population based optimization technique, however, PSO optimizes by adjusting each particle's velocity and position in the searching space in terms of its own experience and the experience of the whole swarm. Saska [5] developed a PSO based path planner, where each path is represented by one particle defined by a set of parameters. Quantum-behaved Particle Swarm Optimization (QPSO) is recognized as an improved version of the original PSO, it assumes that every particle in the swarm has quantum behaviour instead of the conventional position and velocity update rules. Fu applied the QPSO for path planning and compared its performance with the standard PSO in [6].

The ASD scheme is applied in this paper to both GA and PSO based path planners. Monte Carlo simulation results show that the resulting ASD based approach is able to obtain a better optimized result, has faster convergence speed and use less computation time than the unconstrained full space and the circle constrained control point placement methods.

The rest of this paper is organized as follows. Section II provides mathematical models describing the behaviour of static and free moving obstacles, allowing for position uncertainty, and the behaviour of dynamic current flow within an ocean environment, and provides a measure of estimated travel time consumed along a path. Section III outlines the system structure involved in path planning, including path formation and optimization procedures. Section IV introduces previous methods and discusses the proposed approach as well as its integration into the path planner. The Monte Carlo simulation test results are then presented in Section V. The paper ends with concluding remarks in Section VI.

II. PROBLEM FORMULATION

The path planning task is defined by the optimization criteria and the collision constraints, where the optimization criteria are used to obtain the minimum travel time while the collision constraints ensure that the path does not collide with any static or dynamic obstacles.

A. Collision Constraint

1) Obstacles with Fixed Uncertainty

Instead of relying on deterministic analysis based on the assumption of precise knowledge of the obstacles, in this paper, the position uncertainty of the obstacles are modelled with independent Gaussian distribution: $X_o \sim N(\mu_o, \sigma_o^2)$ [7],

Let Γ_k be the location of the vehicle at time k along the path Γ , and $O({\mu_o}^k, {\varpi_o}^k)$ be the circular region of position uncertainty at time k around the obstacle with radius ${\varpi_o}^k$ and centred at ${\mu_o}^k$, where $\varpi_o = 2 \times \sigma_o$ indicates that the probability that the obstacle is located within this region is 95.4%.

2) Obstacles with Propagated Uncertainty

With the assumption that the uncertainty grows linearly with time travelled for this planning horizon, the following model is used to propagate the uncertainty:

$$\varpi_o({\mu_o}^k) = \varpi_o({\mu_o}^{k-1}) + d_{r_o} t({\mu_o}^k, {\mu_o}^{k-1}), \tag{1}$$

where ${\mu_o}^{k-1}$ is the centre of the obstacle at the previous time, d_{r_o} is the uncertainty grows per unit of time traveled, $t({\mu_o}^k, {\mu_o}^{k-1})$ is the time consumed between the two adjacent locations ${\mu_o}^k, {\mu_o}^{k-1}$.

Similarly, the uncertainty at location ${\mu_o}^k$ is defined as:

$$\varpi_o({\mu_o}^k) = \varpi_o({\mu_o}^0) + d_{r_o} t({\mu_o}^k, {\mu_o}^0), \tag{2}$$

where ${\mu_o}^0$ is the initial position of the obstacle, and $t({\mu_o}^k, {\mu_o}^0)$ is the total time taken for the obstacle to move from ${\mu_o}^0$ to ${\mu_o}^k$.

Two forms of obstacle behaviour are considered here. One form is the obstacle remaining static or moving randomly which is fully unpredictable, its centre is assumed to be at its initial location ${\mu_o}^0$, the difference between them is the uncertainty of the latter will grows significantly faster than the former. The second form of obstacle behaviour describes an obstacle moving at a constant velocity and direction from position ${\mu_o}^{k-1}$ to position ${\mu_o}^k$ which is defined as:

$${\mu_o}^k = {\mu_o}^{k-1} + d_{\mu_o} t({\mu_o}^k, {\mu_o}^{k-1}), \tag{3}$$

where d_{μ_o} is the velocity vector of the obstacle.

The following expression imposes the collision value:

$$C = \begin{cases} 1, & S_k \in O({\mu_o}^k, {\varpi_o}^k) \\ 0, & otherwise \end{cases}. \tag{4}$$

B. Optimization Criteria

Time consumption is set as the optimization criteria: the vehicle's thrust power is constant, equivalently, the vehicle's water-referenced speed is constant, and with a given initial point and destination, the objective is to find an optimal path that consumes that consumes the minimum time to travel through a turbulent current field [8].

1) Ocean Field Environment

A turbulent ocean environment with complex currents can be estimated by superposition of multiple located viscous Lamb vortices. The velocity of the current field is represented as $V_c = (u, v)$, where

$$u(\mathbb{R}) = -\eta \frac{y - y_0}{2\pi(\mathbb{R} - \mathbb{R}_o)^2} \left[1 - e^{-\left(\frac{(\mathbb{R} - \mathbb{R}_o)^2}{\zeta^2}\right)} \right], \tag{5}$$

$$v(\mathbb{R}) = \eta \frac{x - x_0}{2\pi(\mathbb{R} - \mathbb{R}_o)^2} \left[1 - e^{-\left(\frac{(\mathbb{R} - \mathbb{R}_o)^2}{\zeta^2}\right)} \right], \tag{6}$$

$\mathbb{R} = (x, y)$ represents the 2-D spatial domain, $\mathbb{R}_o = (x_o, y_o)$ is the center of the vortex and η, ζ are parameters that control the radius and strength of the vortex. In realistic scenarios, the quantity of these Lamb vortices, as well as their positions, radii and intensities may be inferred from current field measurements acquired by a horizontal ADCP (H-ADCP) looking ahead of the AUV [9].

2) Time Consumption

The travelling time T required for a given path is the sum of time t_i required to cover each of these segments constituting the path.

$$T = \sum_1^{\lambda} t_i = \sum_1^{\lambda} \frac{|K_{i-1} - K_i|}{|V_a|}, \tag{7}$$

where λ is the quantity of these path segments, with reference to Fig. 1, V_a is the resultant ground velocity of the vehicle which is resolved using the water-referenced speed of the vehicle in the geographical frame V_r and the velocity of the water current V_c - it can be written as:

$$V_{ay} = |V_r|\, sin\, \psi_r + |V_c|\, sin\, \psi_c\ , \tag{8}$$

$$V_{ax} = |V_r|\, cos\, \psi_r + |V_c|\, cos\, \psi_c\ , \tag{9}$$

where V_{ay}, V_{ax} are the north and east velocity components of the vehicle, respectively.

The resultant ground velocity should orient along the segment $K_{i-1}K_i$ in the direction of the desired motion of the vehicle - it is defined as:

$$\frac{V_{ay}}{V_{ax}} = tan\psi_a = \frac{|y_i - y_{i-1}|}{|x_i - x_{i-1}|}. \tag{10}$$

V_a, ψ_a, t_i are obtained by solving Eq. 8,9,10 as simultaneous equations.

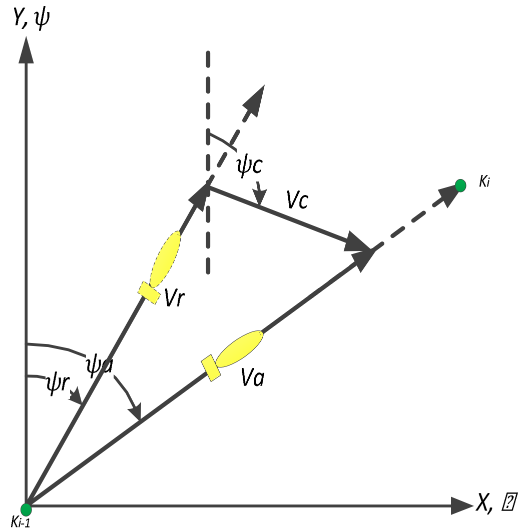

Figure 1. Resultant ground velocity of the vehicle under influence of the ocean current.

The collision constraint is placed as a high-priority objective that will be checked first and its value has to be zero. The evaluation function is defined as:

$$F = \begin{cases} inf, & C = 1 \\ T, & C = 0 \end{cases} \tag{11}$$

III. PATH PLANNING SYSTEM STRUCTURE

A. Path Formation

In the case of an AUV operating in a turbulent ocean environment, the current velocity and the vehicle dynamics impose specific constraints on the achievable smoothness and curvature of the trajectory. In this paper, B-Spline curves are used to define the AUV path. The B-Splines are generated from a set of control points $P = [p_1, \dots, p_i, \dots, p_m]$ that are randomly located in the environment. Every control point $p_i(s, \theta)$ is expressed as log-polar coordinates, where s is the distance of the control point from the initial position and θ is the angle with respect to the north axis.

The path is constructed by connecting a sequence of internal knots K obtained from uniform subdivision which lie between the initial point S and destination point D:

$$\{S, \dots, K_{i-1}, K_i, \dots, D\} \tag{12}$$

It is assumed that any two adjacent knots K_{i-1}, K_i is connected by straight-line segments.

B. Path Optimization

Two path planners, respectively based on the GA and the QPSO methods, are developed here and are used as the platforms to integrate the proposed annulus space decomposition mechanism.

For convenience, the following are defined as common parameters for both the GA and QPSO based path planner: population size ρ (equivalent to the number of candidate paths), dimension of the problem space m (equivalent to the number of path nodes), and maximum number of iterations g.

1) GA Based Path Planner

a) Input the ocean field information and the common parameters: ρ, m, g, as well as the number of genes in each chromosome.

b) Generate an initial group of candidate paths which are represented by the chromosomes, the gene of the i^{th} chromosome at iteration t is represented as:

$$P_i(t) = [p_{i1}(t), p_{i2}(t), \dots, p_{im}(t)]. \tag{13}$$

c) Evaluate the cost function $F(p_i(t))$ of each candidate path (chromosome) as defined in (7).

d) A fraction ∂_e of individuals in the current generation with the best fitness values are called elite children, these individuals automatically survive to the next generation.

e) Selection: A roulette-wheel selection mechanism is applied to stochastically select from one generation to create the mating pool for the next generation. The fitness value $F(p_i(t))$ of each individual is associated with its probability of being selected:

$$Q_i = F(p_i(t)) / \textstyle\sum_{i=1}^{\rho} F(p_i(t)). \tag{14}$$

f) Crossover: children are created by combining the vectors of their parents. A heuristic crossover scheme is applied to the selected chromosomes from the previous step, assuming that $F(p_i(t)) < F\big(p_j(t)\big)$, the new individual is generated by linear combination of their parents, defined as

$$p_i'(t) = \alpha p_i(t) + (1 - \alpha) p_j(t), \tag{15}$$

$$p_j'(t) = p_i(t), \tag{16}$$

where α is a pre-set ratio.

g) Mutation: Mutation creates a random variation of a single parent. The uniform mutation scheme is applied to the remaining individuals, for each mutated individual, a proportion ∂_m of genes are randomly selected and replaced by new genes from the constrained bounds. Let U_j and L_j be the upper and lower bounds, $Rand_{ij}^{M}$ is a random number within the interval $(0,1)$, and $p_{ij}(t)$ is one of the genes selected to be replaced by:

$$p'_{ij}(t) = L_j + \mathrm{Rand}_{ij}^{M}(U_j - L_j). \tag{17}$$

h) Repeat steps (c) to (g) for g iterations or until it reaches the stop criterion.

2) QPSO Based Path Planner

a) Input the ocean field information and choose appropriate parameters for ρ, m, and g.

b) Generate an initial group of candidate paths which are represented by particles with random positions, the position of the i^{th} particle at iteration t is represented as:

$$P_i(t) = [p_{i1}(t), p_{i2}(t), \dots, p_{im}(t)]. \tag{18}$$

c) Initialize the particle's best position, set
$$\mathcal{P}_i(1) = P_i(1).$$

d) Determine the $mbest$, which is defined as the mean of the best positions of all particles:

$$mbest(t) = \textstyle\sum_{i=1}^{\rho} \mathcal{P}_i(t)/\rho\ . \tag{19}$$

e) Evaluate the cost function, $F(p_i(t))$, of each candidate path (particle) as defined in (7).

f) Compare the value of cost function for each particle, $F(\rho_i(t))$, with the best fitness, $F(P_i(t))$:

$$\mathcal{P}_{i+1}(t) = \begin{cases} \mathcal{P}_i(t), & if\ F(p_i) \ge F(\mathcal{P}_i) \\ p_i(t), & if\ F(p_i) < F(\mathcal{P}_i) \end{cases} \tag{20}$$

and the swarm's global best position:

$$G_i = arg\,min\, F(\mathcal{P}_i(t)). \tag{21}$$

g) Update the position of the particle using the following:

$$p_{ij}(t+1) = \delta_{ij}(t) \pm \tfrac{1}{2}\big(L_{ij}(t) ln\ (1/Rand_{ij}^{Up})\big), \tag{22}$$

where $Rand_{ij}^{Up}$ is a random number uniformly distributed within the interval (0,1), $\delta_{ij}(t)$ is a local attractor defined as:

$$\delta_{ij}(t) = Rand_{ij}^{U\delta}\mathcal{P}_{ij}(t) + (1 - Rand_{ij}^{U\delta})G_{ij}(t) \tag{23}$$

where $Rand_{ij}^{U\delta}$ is a random number uniformly distributed within the interval $(0,1)$.
Parameter $L_{ij}(t)$ is evaluated by:

$$L_{ij}(t) = 2\beta\left|mbest_j(t) - p_{ij}(t)\right| \tag{24}$$

where β is the parameter which controls the convergence speed of the algorithm.

h) Repeat step (c) to (g) for g iterations or until it reaches the stop criterion.

IV. Annular Space Decomposition mechanism

A. Existing Control Point Placement Mechanisms

1) Unconstrained Searching

The fully unconstrained space (FS) searching mechanism is the original method which allows the control points to be freely located in the environment. In this case, the control point is defined as $p_{ij}(s_{ij}, \theta_{ij})$ where

$$s_{ij} = Rand_{ij}^{Fs}\, l\ , \tag{25}$$

$$\theta_{ij} = Rand_{ij}^{F\theta}\,(\tfrac{\pi}{2})\ , \tag{26}$$

l is the length of the straight line connecting the initial and destination points, $Rand_{ij}^{Fs}$ and $Rand_{ij}^{F\theta}$ are random numbers between $(0,1)$.

2) Concentric Circles (CC) Space Decomposition

The concentric circles space decomposition mechanism reduces computation time by constraining the control points to lie on deterministically spaced concentric circles, one point per circle, radiating out from the start point to the destination.

The radii of the concentric circles $E = [r_1, \dots, r_i, \dots, r_m]$ are generated as follow:

$$r_i = \left(\tfrac{i}{m+1}\right) l \qquad i = 1, \dots, m\ . \tag{27}$$

In this case, each control point is defined as $p_{ij}(s_{ij}, \theta_{ij})$, where

$$s_{ij} = r_i\ , \tag{28}$$

$$\theta_{ij} = Rand_{ij}^{C\theta}\,(\tfrac{\pi}{2})\ . \tag{29}$$

B. Annular Space Decomposition (ASD)

The ASD mechanism decomposes the search space into a sequence of evenly spaced concentric annuli with one or more control points located per annulus. The annuli are formed by the space between every pair of adjacent concentric circles of radii r_{i-1} and r_i, where

$$r_i = \left(\frac{i}{\omega}\right) l \qquad i = 1, \dots, \omega \tag{30}$$

The parameter ω is obtained from:

$$\omega = \frac{m}{q} \quad (31)$$

where m is the number of control points set to generate the Spline curved path and q is the number of control point allowed within each annulus.

C. ASD based Path Optimization Algorithms

1) Bound Constraints

Two constraints need to be satisfied throughout the optimization, one is the bound of s_{ij}: $[LS, US]$and the other is the bound of θ_{ij}: $[L\theta, U\theta]$ – these bounds are defined as:

$$LS = [0, r_1, \dots r_{i-1}, \dots r_{m-1}], \quad (32)$$

$$US = [r_1, r_2, \dots r_i, \dots r_m], \quad (33)$$

$$L\theta = [0,0, \dots ,0, \dots ,0], \quad (34)$$

$$U\theta = [\tfrac{\pi}{2}, \tfrac{\pi}{2}, \dots , \tfrac{\pi}{2}, \dots , \tfrac{\pi}{2}]. \quad (35)$$

2) Constrained Optimization

a) GA-ASD

The GA is initialized to have a population size of ρ candidate paths, each path is generated from m control points which are dispersed over ω annuli, with q control points per annulus, thus the initial population $P(1)$ is prepared by randomly generating $q \times \rho$ points within each annulus, where each point $p_{ij}(s_{ij}, \theta_{ij})$ is generated from:

$$s_{ij} = LS_j + Rand_{ij}^{As}(US_j - LS_j) \quad (36)$$

$$\theta_{ij} = Rand_{ij}^{A\theta}(U\theta_j - L\theta_j) \quad (37)$$

where $i = 1, \dots , \rho$ and $j = 1, \dots , m$ and $Rand_{ij}^{As}$ and $Rand_{ij}^{A\theta}$ are random numbers within the interval $(0,1)$.

GA uses mutation and crossover functions to produce new individuals at every generation. Constraints bounds applied to these functions ensure that only feasible points are generated.

b) QPSO-ASD

For QPSO-ASD, the population initialization process is similar to that of GA-ASD except that it adds one more step after the position update to check if the new particle position is within bounds. The following expression ensures that every dimension of the updated particle meets its constraints:

$$p_{ij}(t+1) = \begin{cases} p_{ij}(t+1), & if\ s_{ij} \in (LS_j, US_j) \cap \theta_{ij} \in (\theta S_j, \theta S_j) \\ p'_{ij}(t+1), & otherwise \end{cases} \quad (38)$$

where $p'_{ij}(t+1)$ is a randomly generated particle from Eq. 16.

V. SIMULATION RESULT

A. Simulation Setup

The FS, CC and ASD mechanisms are integrated in both GA and QPSO based path planners and implemented in Matlab.

As mentioned in Section II-B, the current field for the scenario reported in this paper, is generated from a random distribution of 50 Lamb vortexes within a 2-D spatial domain represented by a 100 × 100 grid. The distance between neighbouring grid points corresponds to 1000 m. The strength ζ and radius η of each vortex are set as 15 and 2, respectively. The water-referenced speed of the vehicle in the geographical frame is set at 5 m/s. The initial and destination points are located at grid locations (1,1) and (60,80), respectively. Each B-Spline curved path is uniformly subdivided by 1152 internal knots.

In order to allow consistent evaluation across the path planners, common parameters are used for both GA and QPSO: i.e., population size is 200, each individual path has 12 control points and the maximum number of iterations is 100. In addition, each algorithm has its own specific parameters. For GA, 80% of the population other than the elite individuals will be selected for crossover; the parameter for the heuristic crossover is 1.2; for each mutated individual, the mutation probability of its gene is 0.01; For QPSO, the contract-expansion coefficient β is set to linearly decrease from 1.0 to 0.5 over the 100 iterations. For simplicity, 12 annuli were generated for the ASD based path planner such that only one control node is located within each annulus.

B. Currents Field with Obstacles of Fixed Uncertainty

For comparison purposes, the optimal path projections obtained for each scheme GA-FS (blue line), GA-CC (black line), GA-ASD (red line) are shown in Fig. 2(a). Three obstacles with fixed position uncertainty are modelled as Gaussian distributions: $X_{o1} \sim N(15,20)$, $X_{o2} \sim N(48,49)$ and $X_{o3} \sim N(60,75)$, respectively, the black circles with radius of $2\sigma_o$ represent a confidence of 95.4% that the obstacle will be located within this area. The relationship between the best fitness value and the number of iterations is show in Fig. 2(b).

Similar experiments are also done for the QPSO based path planner. The results for the QPSO are shown as Fig. 3.

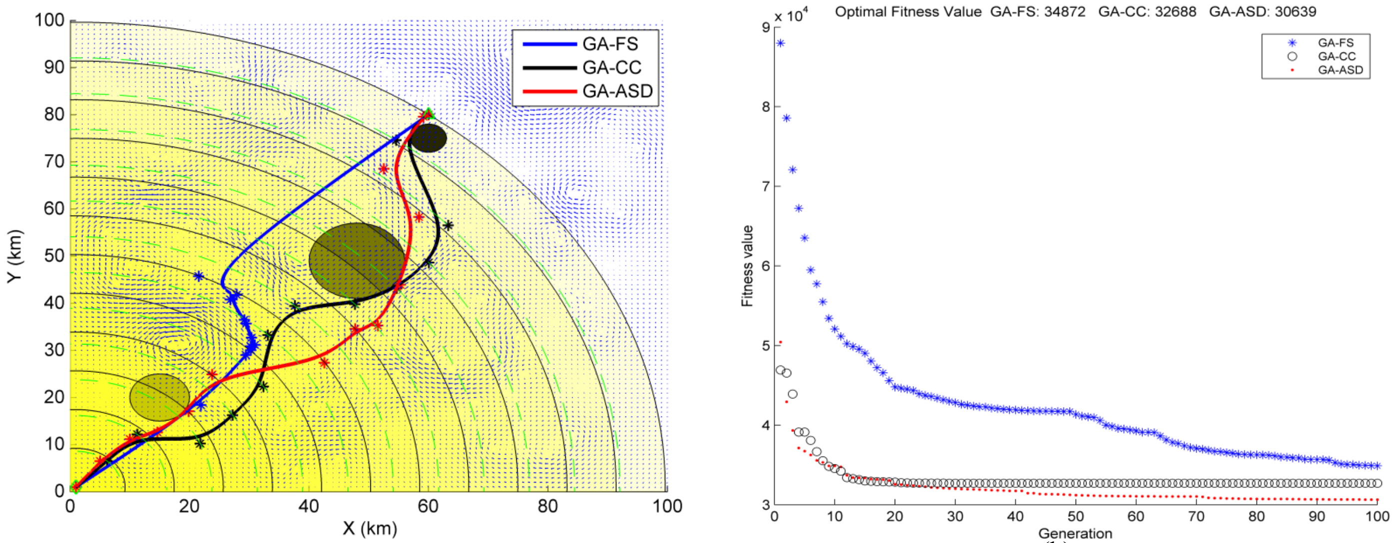

(a) (b)

Figure 2. Comparison of results produced by the FS, CC and ASD schemes with the GA path planner for static obstacles: (a) path projections in the 2D current field, (b) convergence curve of best fitness values.

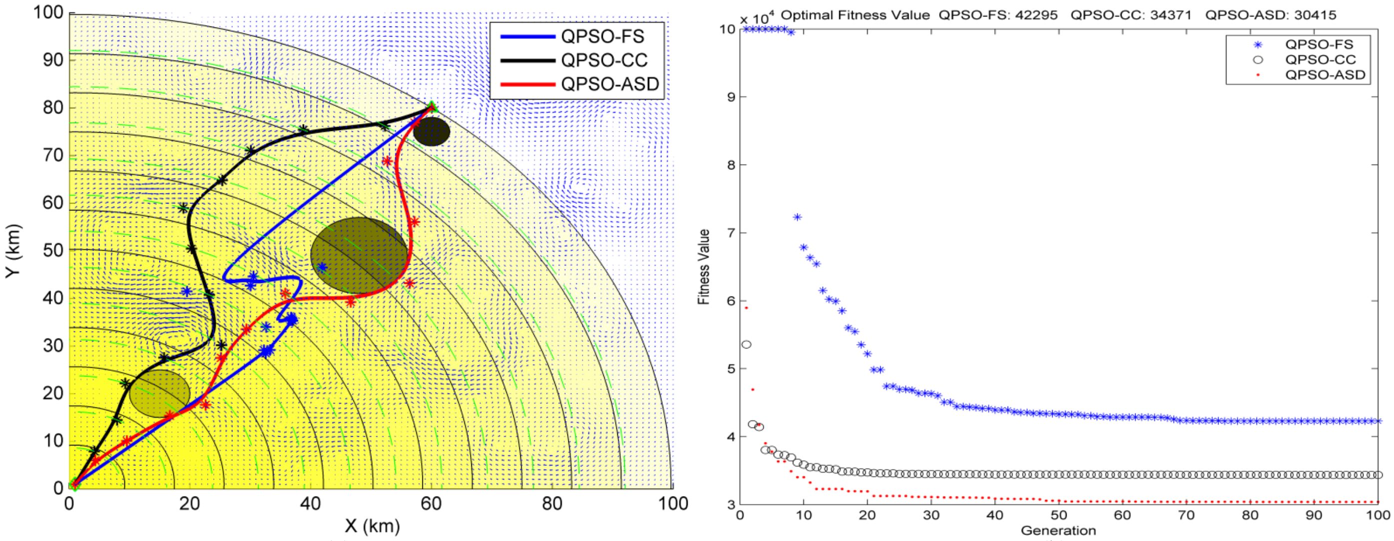

(a) (b)

Figure 3. Comparison of results produced by the FS, CC and ASD schemes with the QPSO path planner for static obstacles: (a) path projections in the 2D current field, (b) convergence curve of best fitness values.

It can be seen from Fig. 2 and Fig. 3 that the FS scheme, for both the GA and the QPSO path planner, allows control points to cluster closely which leads to redundant searching, while in the case of the CC and ASD schemes, the control points are spread out over the whole search space, thus avoiding misplaced effort. The penalty for the redundant searching incurred by the FS scheme is clearly seen in Figs. 2(b) and 3(b), which shows the slow rate of convergence for the FS scheme relative to the ASD and CC schemes.

It is also evident from Figs. 2(b) and 3(b) that the proposed ASM scheme achieves more optimal results than the CC and FS schemes. The reasons can be found from Figs. 2(a) and 3(a). In the CC scheme, every control point is constrained to move along the circumference of its respective concentric circle, while in contrast, the ASD scheme permits more flexibility to search around obstacles and generate more complex shaped paths which reduces travel distance. Theoretically, the FS scheme also enjoys similar flexibility to the ASD scheme and has the potential to construct complex shaped paths, however, because of its potential for overlapped searching, it is more likely to become stuck at a local minima.

C. Currents Field with Obstacles of Propagated Uncertainty

Similar simulations but with obstacles of propagated uncertainty have also been conducted. As mentioned in Section II-C, two cases are studied here.

1) Static or Unpredictable Obstacles

The positions of two obstacles are modelled as Gaussian distributions, with initial condition $X_{o1} \sim N(20,20)$, $X_{o2} \sim N(35,45)$, respectively. It is assumed the region of uncertainty around the obstacle position grows linearly with the time travelled, this is related to the growth of the variance, and is expressed in Fig. 4(a-c) as the radius of the circle growing at a rate of 0.1 m/s of time travelled. The different colours represent the position uncertainty of obstacles at different time. Note that the optimal curve obtained from QPSO-ASD is also represented by a changing colour, this colour reflects the associated travelling time of the vehicle when following the path. At the any discrete time point, the obstacle and the path node are represented by the same colour, thus if this node is not inside the obstacle boundary, no collision will occur.

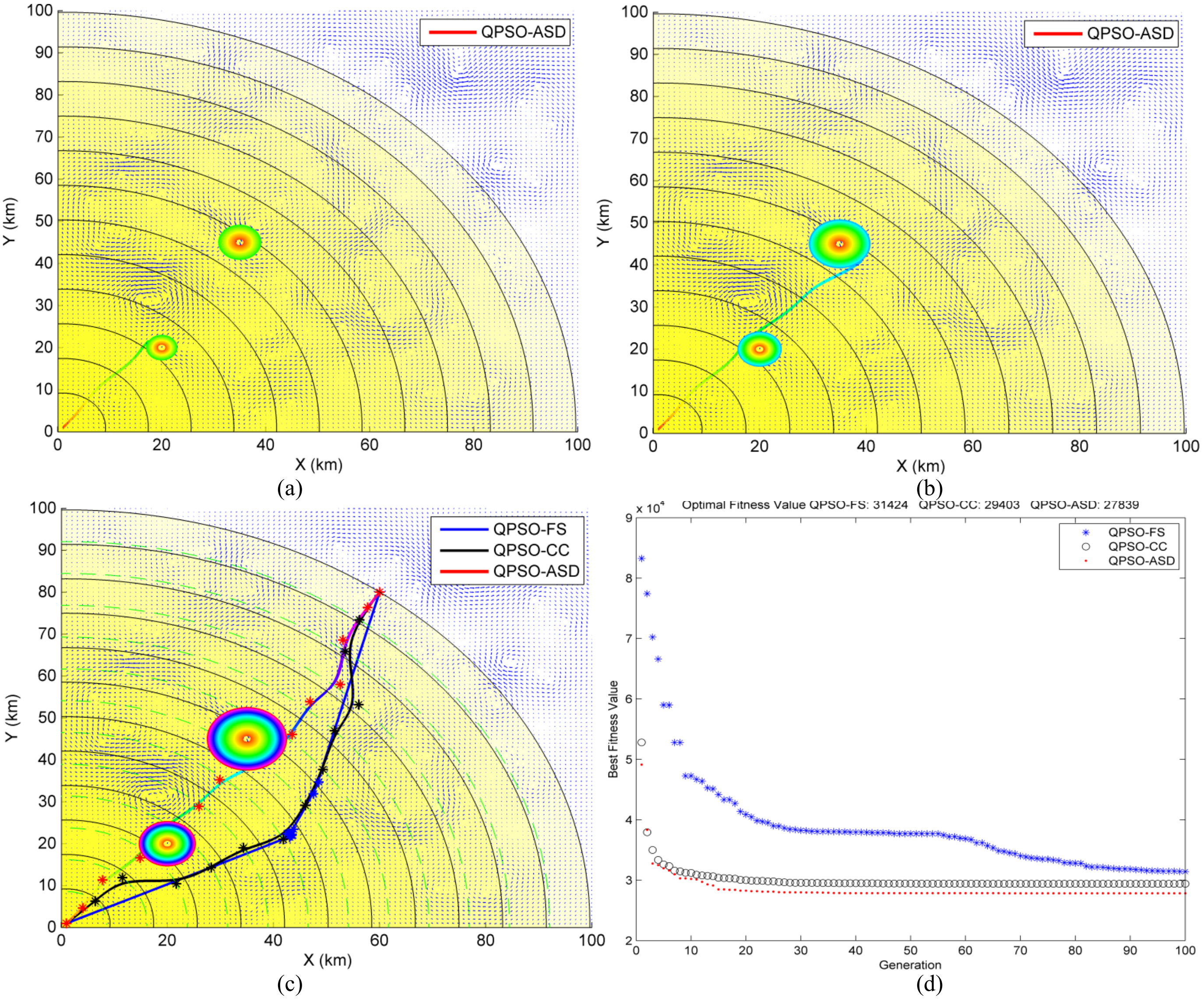

Figure 4. Comparison of results produced by the FS, CC and ASD schemes with the QPSO path planner for static obstacles of propagated uncertainty: (a)-(c) Path projections in the 2D current field. (d) Convergence curve of best fitness values.

2) Constantly Moving Obstacles

Little modification to the previous model is needed to model the obstacles as constantly moving with increasing uncertainty. The obstacles are modeled as Gaussian distributions, with initial condition $X_{o1} \sim N(20,15)$, $X_{o2} \sim N(60,40)$ respectively. Their centers are configured to move independently at a rate of 1 m/s northwards and 3 m/s eastwards, respectively.

The simulation results displayed in Fig. 4 and Fig. 5 demonstrate that the ASD scheme maintains its superiority compared with the FS and CC schemes for both GA and QPSO based path planner in both scenarios with static or constantly moving obstacles of propagated uncertainty.

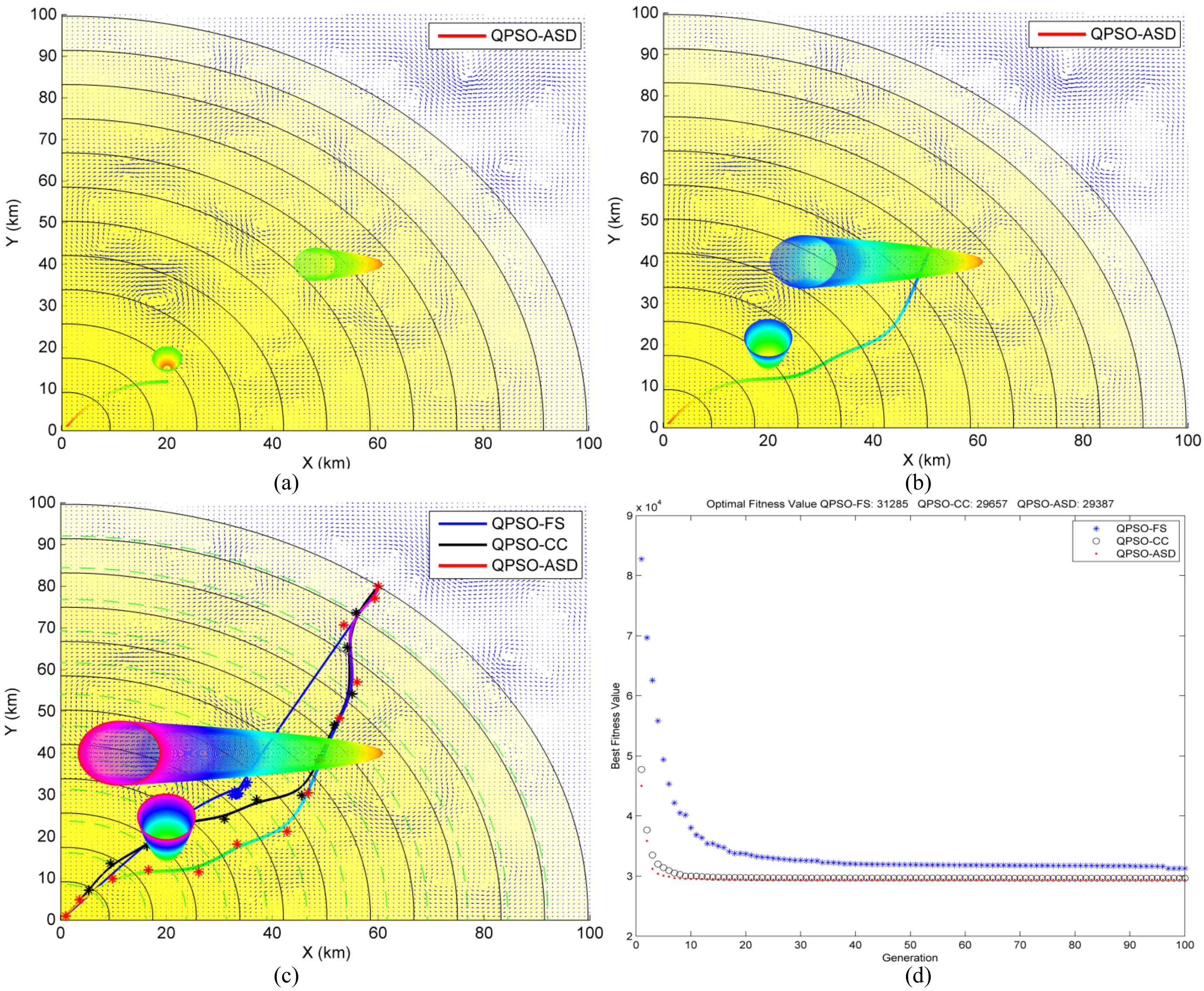

Figure 5. Comparison of results produced by the FS, CC and ASD schemes with the QPSO path planner for constantly moving obstacles of propagated uncertainty: (a)-(c) Path projections in the 2D current field. (d) Convergence curve of best fitness values.

D. Robustness Assessment

Monte Carlo simulation runs are conducted to assess the robustness of each path planning method. The simulation is repeated for a 100 runs, the settings for each run are mostly the same as those used in Section V-A, except that no obstacles are included in this scenario and a stopping criteria E is added which allows the simulation to terminate early if this criteria is achieved. The simulation stops when E, which is defined as the weighted average change in the fitness function value over certain generations (5 generations in these simulations), is less than the function tolerance (1×10^{-6}).

$$E = \sum_{i=1}^{5} (((F_{I-i}(t) - F_{I-i-1}(t))/F_{I-i}(t))\,(0.5)^{i-1} \qquad (39)$$

where i is the number of the latest iteration, F is the relevant fitness value.

The performances of the FS, CC and ASD schemes are compared based on the following three factors: searching ability, convergence speed and computation time. The searching ability can be evaluated by the searching quality (mean best fitness value) and the stability - as the proposed optimization is a minimization problem, the smaller the mean value, the stronger the searching ability. The stability is expressed as a standard deviation. The convergence speed reveals how fast the algorithm converges to the optimal solution. Computation time is the mean CPU time usage over 100 runs for each strategy. From the statistical results presented in Table I and Table II, for both the GA and QPSO based path planner, it can be seen that the ASD approach is able to obtain a more optimized trajectory than the CC method, and has faster convergence speed and use less computation time than the FS method.

Comparing the results in Tables I and II for the GA and QPSO algorithms, respectively, it can be seen that, QPSO converges significantly faster with lower computation consumption than GA for this simulation scenario. Although the GA-ASD is considerably slower than the QPSO-ASD, it eventually produces better and more robust trajectories, as indicated by the lower fitness value, and the significantly smaller standard deviation after about 100 iterations.

TABLE I. PERFORMANCE COMPARISON OF FS, CC, ASD SCHEMES ON GA BASED PATH PLANNER

Algorithm	Best Fitness		Convergence Generation		Computation Time (sec)	
	Mean	***Std***	***Mean***	***Std***	***Mean***	***Std***
GA-FS	2.7815e+04	4.9960e+02	1.8601e+02	23.2128	1.5031e+03	3.13888e+02
GA-CC	2.7776e+04	5.5883e+02	67.87	22.6976	5.4768e+02	1.9262e+02
GA-ASD	2.7377e+04	21.3140	1.0042e+02	25.0236	8.1143e+02	2.4851e+02

TABLE II. PERFORMANCE COMPARISON OF FS, CC, ASD SCHEMES ON QPSO BASED PATH PLANNER

Algorithm	Best Fitness		Convergence Generation		Computation Time (sec)	
	Mean	***Std***	***Mean***	***Std***	***Mean***	***Std***
GA-FS	2.7937e+04	7.4722e+02	1.1025e+02	38.6019	4.0789e+02	1.4603e+02
QPSO-CC	2.7638e+04	4.7629e+02	53.70	11.8904	1.9816e+02	43.8151
QPSO-ASD	2.7516e+04	3.4254e+02	51.32	12.5101	1.9054e+02	48.1159

VI. CONCLUSIONS

A novel annular space decomposition (ASD) scheme, and its subsequent integration with the GA and QPSO based path planners has been proposed and discussed in this paper. Simulation tests have been done to generate an optimal trajectory with minimum time consumption for an AUV travelling through a turbulent ocean fields in the presence of obstacles with position uncertainty. Based on the results from these tests, the ASD scheme is shown to be capable of achieving a more optimized trajectory than the circle constrained method, and has faster convergence speed and uses less computation time than the fully unconstrained method. Monte Carlo simulations demonstrate the robustness and superiority of the proposed ASD scheme comparing with the previous methods.

ACKNOWLEDGMENT

Zheng Zeng postgraduate scholarship is provided by the China Scholarship Council and the Flinders University scholarship program. The research is funded through a CSIRO Wealth from Oceans program.

REFERENCES

[1] A. Alvarez, A. Caiti, and R. Onken, "Evolutionary path planning for autonomous underwater vehicles in a variable ocean," IEEE Journal of Oceanic Engineering vol. 29, pp. 418-429, 2004.

[2] C. Zheng, L. Li, F. Xu, F. Sun, and M. Ding, "Evolutionary route planner for unmanned air vehicles," IEEE Transactions on Robotics, vol. 21, pp. 609-620, 2005.

[3] I. K. Nikolos, K. P. Valavanis, N. C. Tsourveloudis, and A. N. Kostaras, "Evolutionary algorithm based offline/online path planner for UAV navigation," IEEE Transactions on Systems, Man, and Cybernetics, Part B: Cybernetics, vol. 33, pp. 898-912, 2003.

[4] H. Yanling, Z. Wei, and Z. Yuxin, "Real-time obstacle avoidance method based on polar coordination particle swarm optimization in dynamic environment," 2007 2nd IEEE Conference on Industrial Electronics and Applications, 2007. ICIEA, 2007. pp. 1612-1617.

[5] M. Saska, M. Macas, L. Preucil, and L. Lhotska, "Robot path planning using particle swarm optimization of ferguson splines," IEEE Conference on Emerging Technologies and Factory Automation, 2006. ETFA '06,2006, pp. 833-839.

[6] F. Yangguang, D. Mingyue, and Z. Chengping, "Phase angle-encoded and quantum-behaved particle swarm optimization applied to three-dimensional route planning for UAV," IEEE Transactions on Systems, Man and Cybernetics, Part A: Systems and Humans, vol. 42, pp. 511-526, 2012.

[7] J. P. Gonzalez and A. Stentz, "Planning with uncertainty in position an optimal and efficient planner," 2005 IEEE/RSJ International Conference on Intelligent Robots and Systems, 2005. (IROS 2005). 2005, pp. 2435-2442.

[8] B. Garau, A. Alvarez, and G. Oliver, "Path planning of autonomous underwater vehicles in current fields with complex spatial variability: an A* approach," Proceedings of the 2005 IEEE International Conference on Robotics and Automation, 2005. ICRA 2005. 2005, pp. 194-198.

[9] B. Garau, A. Alvarez, and G. Oliver, "AUV navigation through turbulent ocean environments supported by onboard H-ADCP," Proceedings 2006 IEEE International Conference on Robotics and Automation, 2006. ICRA 2006. 2006, pp. 3556-3561.